Naval Research Laboratory

Washington, DC 20375-5000

DTIC FILE COPY

NRL Report 9030

AD-A179 402

Wideband Parallel-Plate Waveguide, Phased-Array Antenna

J. B. L. RAO S. R. LAXPATI, AND B. D. WRIGHT

Electromagnetics Branch
Radar Division

February 13, 1987

DTIC ELECTE APR 2 1 1987 S D E

Approved for public release, distribution unlimited

2

SECURITY CLASSIFICATION OF THIS PAGE

REPORT DOCUMENTATION PAGE

AD-A179402

1a REPORT SECURITY CLASSIFICATION UNCLASSIFIED	1b RESTRICTIVE MARKINGS
2a SECURITY CLASSIFICATION AUTHORITY	3 DISTRIBUTION/AVAILABILITY OF REPORT Approved for public release; distribution unlimited.
2b DECLASSIFICATION/DOWNGRADING SCHEDULE	
4 PERFORMING ORGANIZATION REPORT NUMBER(S) NRL Report 9030	5 MONITORING ORGANIZATION REPORT NUMBER(S)
6a NAME OF PERFORMING ORGANIZATION Naval Research Laboratory 6b OFFICE SYMBOL (If applicable) Code 5372	7a NAME OF MONITORING ORGANIZATION
6c ADDRESS (City, State, and ZIP Code) Washington, DC 20375-5000	7b ADDRESS (City, State, and ZIP Code)
8a NAME OF FUNDING/SPONSORING ORGANIZATION Office of Naval Research 8b OFFICE SYMBOL (If applicable)	9 PROCUREMENT INSTRUMENT IDENTIFICATION NUMBER
8c ADDRESS (City, State, and ZIP Code) Arlington, VA 22217	10 SOURCE OF FUNDING NUMBERS PROGRAM ELEMENT NO: 61153N PROJECT NO: RR021-05-43 TASK NO: WORK UNIT ACCESSION NO: DN380-049

11 TITLE (Include Security Classification)
Wideband Parallel-Plate Waveguide, Phased-Array Antenna

12 PERSONAL AUTHOR(S)
Rao, J. B. L., Laxpati, S. R., and Wright, B. D.

13a TYPE OF REPORT	13b TIME COVERED	14 DATE OF REPORT (Year, Month, Day)	15 PAGE COUNT
Final	FROM _____ TO _____	1987 February 13	25

16 SUPPLEMENTARY NOTATION

17 COSATI CODES		
FIELD	GROUP	SUB-GROUP

18 SUBJECT TERMS (Continue on reverse if necessary and identify by block number)
Phased arrays; Aperture matching; Waveguide simulators; Wide bandwidth; Parallel-plate waveguides; Active element pattern; Experimental studies

19 ABSTRACT (Continue on reverse if necessary and identify by block number)

A need exists for wideband phased-array radars. This report presents the results of some experimental studies made on improving bandwidth and scanning-range performance of phased-array antennas. A parallel-plate waveguide element, operating in the S-band (2.8 to 4.2 GHz) was used as the radiating element. Such an element permitted the needed less than one-half wavelength interelement spacing for broadband applications and has been found to provide good aperture matching for H-plane scanning. The element is fed by a broadband, end-on, base-fed, coaxial-to-waveguide transition. H-plane waveguide simulators have been used to study aperture match performance and to optimize array parameters to improve bandwidth and scan range. The waveguide simulator results showed that a good aperture match, with voltage standing wave ratio (VSWR) of about 2:1 over a 40% bandwidth and ±60° scan angle, is achievable for H-plane scanning. Experimentally optimized array parameters are then used to build an 11 × 11 element array. The scanning performance of that array in H- and E-planes was studied by measuring active element patterns. This does not give precise results, but did show that the aperture match is about equally good, over ±60° and 40% bandwidth, for H- and E-plane scanning.

20 DISTRIBUTION/AVAILABILITY OF ABSTRACT	21 ABSTRACT SECURITY CLASSIFICATION
☐ UNCLASSIFIED/UNLIMITED ☒ SAME AS RPT ☐ DTIC USERS	UNCLASSIFIED

22a NAME OF RESPONSIBLE INDIVIDUAL	22b TELEPHONE (Include Area Code)	22c OFFICE SYMBOL
J. B. L. Rao	(202) 767-2584	Code 5372

DD FORM 1473, 84 MAR 83 APR edition may be used until exhausted
All other editions are obsolete

SECURITY CLASSIFICATION OF THIS PAGE

CONTENTS

Accession For
NTIS GRA&I
DTIC TAB
Unannounced
Justification
By
Distribution/
Availability Codes
Dist | Avail and/or Special
A-1

QUALITY INSPECTED 1

WIDEBAND PARALLEL-PLATE WAVEGUIDE, PHASED-ARRAY ANTENNA

INTRODUCTION

Phased-array antennas have been studied for well over two decades. Many authors have reported on analytical as well as experimental phased-array work. References 1 through 5 provide a good overview of this subject through 1970. Microstrip and microwave integrated circuit (MIC) technology have provided a renewed impetus to the phased-array studies [6]. Numerous papers have been published in the last few years on the subject of phased arrays using microstrip elements. It is quite evident from the published literature that the primary concern of the researchers in this field remains with the understanding of mutual coupling effects between array elements, and its impact on the performance of the array, over the scan range and the frequency band.

An aspect of phased-array antennas that still remains of significant importance is the impedance matching of an array over a fairly large frequency band (40% or more) and with a wide angle (conical) scan (coverage of $\pm 60°$ or more). Several analytical studies and some experimental work on this particular aspect have been reported (see bibliography on WAIM-Phased Arrays).* However, only limited data are available on broadband, wide angle scanned arrays. Thus, it is of considerable interest to investigate both theoretically and experimentally, the design and development of a broadband, wide angle scanned phased array. Some theoretical studies were reported [7] for a simpler configuration. This report discusses the experimental work conducted at NRL. The next section discusses the general design specification of the phased array followed by the development of specifications of various waveguide simulators. Experimental results are then presented for three H-plane simulators. The results show that good aperture match, with voltage standing wave ratio (VSWR) of ≤ 2.1 over a 40% bandwidth is achievable for H-plane scanning. Finally, a brief discussion is included on an 11 × 11 element array that was built to verify the scanning performance for E- as well as H-plane scanning by measuring active element patterns. The measured results show that the aperture match is equally good, over $\pm 60°$ scanning and over 40% bandwidth, for scanning in both planes. An extensive bibliography of the phased array literature is also included.

PRELIMINARY ARRAY DESIGN

Based on the general specifications of the phased array, the following specifics were settled on at an early stage.

Operating frequency band: S-band (2 to 4 GHz)
Square array grid of elements
Bandwidth = 40%
Maximum scan angle $\theta_{max} = 60°$.

A square grid was chosen because it is the simplest and for waveguide simulation it may be more convenient.

Manuscript approved October 31, 1986.
*Wide-Angle Impedance Matching (WAIM).

From the bandwidth and θ_{max} specifications, the element spacing d can be readily determined from

$$\frac{d}{\lambda} \leqq \frac{1}{1 + |\sin \theta_{max}|} . \tag{1}$$

Equation (1), where λ is the wavelength, ensures that no grating lobe maxima appear. If f_0 is the center frequency, the operating frequency band for a 40% bandwidth is 0.8 to 1.2 f_0. Then, using Eq. (1), one can readily determine that d/λ_0 must be less than 0.45. Thus, an element spacing of $d/\lambda = 0.4$ was picked. Note that λ_0 is the wavelength at frequency f_0.

The choice of f_0 within the S-band is quite arbitrary. It was picked as 3.5 GHz to facilitate the waveguide simulator design as discussed in the following section.

The preliminary array design specifications, in addition to those delineated above, now include:

Operating frequency band : 2.8 to 4.2 GHz
Center frequency f_0: 3.5 GHz
Element spacing d: 0.4 λ_0.

DESIGN OF WAVEGUIDE SIMULATORS

The performance of a phased array is strongly influenced by the mutual coupling between its elements. This effect manifests itself as variations in the impedance of the array as a function of scan direction. It is conveniently represented as a variation of active impedance or as an element gain pattern. However, measurement of either of these quantities requires the construction of the entire array. An alternative to this expensive proposition is the use of waveguide simulators that can effectively simulate an infinite array to determine the impedance match of the elements in the actual (infinite) array environment.

The design principles of waveguide simulators have been treated in detail by Hannan and Balfour [8] and Wheeler [9]. Following these references, a set of simulators for H-plane scan, E-plane scan, and intercardinal (IC) plane scan can be designed. Each of the simulators will simulate a specific scan angle at a given frequency. Thus, limited scan coverage can be obtained from each simulator by varying the operating frequency. A proper choice of the simulators could then provide almost complete scan-range simulation with a limited number of simulators; this is particularly true for the wideband elements required in this project.

Figure 1 shows a square grid array with elements represented by circles. Also shown are several H-plane simulator geometries. That each one of these simulators will simulate an infinite array is obvious from simple image principles. These simulators must operate in TE_{10} mode to simulate H-plane scan. This can be readily verified by decomposing the TE_{10} mode in a waveguide in terms of two plane waves at an angle θ_s with respect to the axis of the simulator. The relationship between the simulator dimensions and the scan angle θ_s is:

$$\text{For H-plane scan:} \quad p\frac{d}{\lambda} \sin \theta_s = 1 \tag{2a}$$

$$\text{For IC-plane scan:} \quad p\frac{d}{\lambda} \sin \theta_s = 1/\sqrt{2} \tag{2b}$$

where p is an integer and d is the element spacing in the square grid. The corresponding simulator dimensions are:

$$\text{H-plane:} \quad pd/2 \times d$$

$$\text{IC-plane:} \quad pd/\sqrt{2} \times d/\sqrt{2}.$$

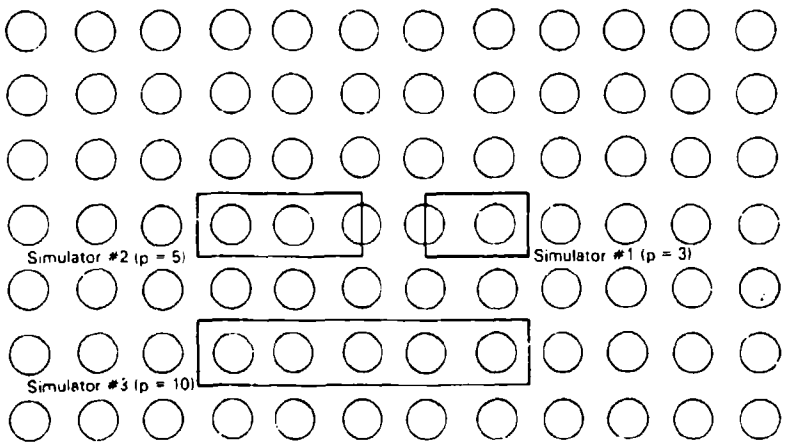

Fig. 1 — H-plane simulators in a square grid array; $p = 3, 5$, and 10

The number of array elements needed for the simulator depends also on the scan angle. In Table 1, the scan angles and the number of elements are tabulated for different values of p for H-plane simulators. A value of $d/\lambda_0 = 0.4$ is assumed at the center frequency f_0. In practice, it should be noted that often fractional elements may be omitted with negligible error in the results of simulation.

Table 1 — Scan Angle and No. of Elements for H-Plane Simulators for $d/\lambda = 0.4$

Waveguide Dimension $\left(\frac{pd}{2} \times d\right)$

p	Scan Angle θ_s (deg)	No. of Elements
3	56	1-1/2
4	39	2
5	30	2-1/2
6	25	3
7	21	3-1/2
8	18	4
9	16	4-1/2
10	15	5

Figure 1 shows the three H-plane simulators proposed for this task. They correspond to $p = 3, 5$, and 10.

A range of scan angles can be simulated by variation of the frequency in each of the simulators. Figure 2 shows the plot of the scan angle vs frequency for the three simulators. Note that Simulator #1 ($p = 3$) should not be operated below 3.0 GHz, since it has the TE_{10} mode cutoff frequency of 2.94 GHz. Also, the three simulators together over the 2.8 to 4.2 GHz band provide almost continuous scan coverage from 12° to 78°. Simulation below 12° would require an increasingly larger size simulator and a corresponding increase in the number of elements. Fortunately, the element gain patterns are usually broad and thus, only a small change in the pattern occurs over 0° to 12°. Thus, it is not necessary to simulate the array at broadside (the 0° scan angle).

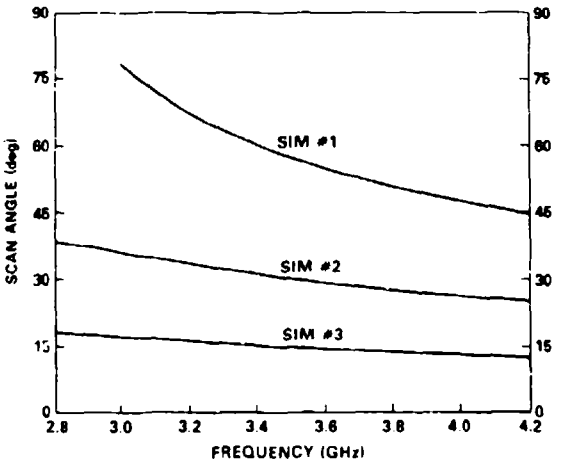

Fig. 2 — Scan angle vs frequency for various simulators

ARRAY ELEMENT

An important aspect of the development of a phased-array system is the selection of an element. Many radiating elements are suitable for a phased array; however, the most frequently used elements are dipoles, slots, and waveguides because of their simplicity. Another advantage of using one of these elements is that the mutual coupling effect has been extensively investigated by many workers. Slot and dipole elements are quite suitable for microstrip and MIC technology.

The present project, because of its wideband requirement, places a constraint on the selection of an element. Waveguides, whether rectangular, circular, or square in cross section, are suitable for wideband operation. But, since the element spacing is less than one-half wavelength, in a square grid arrangement, the waveguides must be dielectric filled in order to reduce their physical size to meet the array spacing. Fortunately, a parallel-plate waveguide may be used as a radiator for the phased-array. Such an element is simple, has wide bandwidth, and does not require dielectric loading to meet the 0.4λ element spacing in square grid. Also, as reported by Davis et al. [10] and Hrycak [11], a parallel-plate waveguide element fed by a stripline performs satisfactorily in a phased-array environment. Thus, it was decided to use a parallel-plate waveguide radiator element.

Parallel-Plate Waveguide Element

The element spacing at the center frequency (3.5 GHz) is 1.34 in. (0.4λ). Thus, the parallel plates must have a separation of almost 1.34 in. Since the standard S-band waveguide E-plane dimension is also 1.34 in., size of the parallel-plate waveguide was chosen to be the same. This waveguide must be fed at an interval of 1.34 in. Since, in the planar array, the parallel-plate elements will be stacked, the feed cannot be located at the top or the bottom. It must be fed from the back wall of the guide. If it is fed in the center of this wall by using a strip line, because of the low impedance of the feed, a wideband impedance transformer would be necessary. To circumvent this, the chosen feed is a probe antenna that is fed by a coaxial cable that is located near the bottom of the back wall. This end-feed arrangement in a rectangular waveguide would excite TE_{10} mode. Figure 3 shows the detailed geometry of the parallel-plate waveguide element.

The dimensions shown for the probe in an S-band waveguide were arrived at experimentally. The probe dimensions were optimized to give a low VSWR (less than 1.4) over the 2.8 to 4.2 GHz band. Although a better match could be obtained, it was not deemed necessary since the probe will be spaced closer in the parallel-plate waveguide than the equivalent spacing in the S-band guide obtained through the image principle.

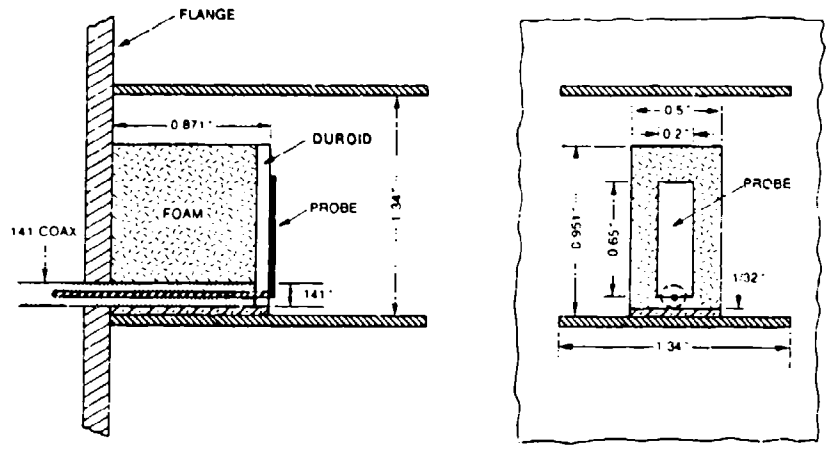

Fig. 3 — Detailed geometry of the end-on, bottom-fed probe

The end-on, bottom fed probe for the parallel-plate waveguide element has several advantages. First, it is simple to build and thus readily reproduced in a laboratory. Also, by adjusting its parameters, it is possible, in principle, to avoid an impedance transformer.

EXPERIMENTAL RESULTS

As stated in the previous sections, probe-fed, parallel-plate waveguides are used as the radiating elements of a phased array. The probe dimensions are optimized to give a low VSWR in a waveguide over a 2.8 to 4.2 GHz range. The optimized dimensions were shown in Fig. 3. Figure 4 shows the input VSWR of that probe in S-band waveguide. It is clear that this VSWR is less than 1.4 over a broad frequency range

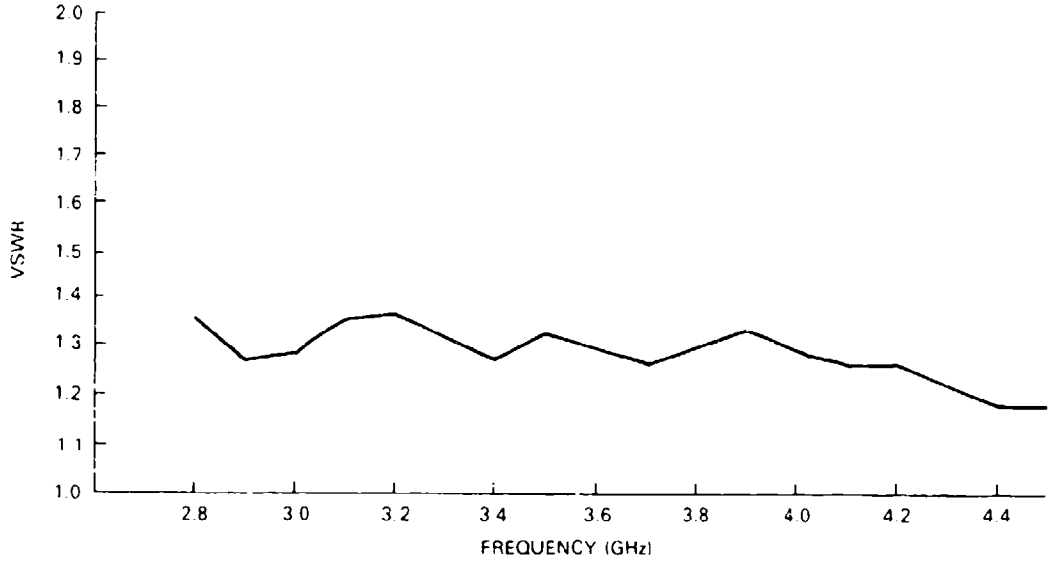

Fig. 4 — Input VSWR of a coaxial probe in a S-band waveguide vs frequency

As a starting point, the above optimized probed dimensions are used in waveguide-simulator experiments. The probe dimensions are then optimized to reduce VSWR to the lowest level over the frequency range of interest for all three H-plane simulators.

H-Plane Waveguide Simulators

A simulator is made up of a waveguide (here called a simulator waveguide) terminated in a section of the array containing a small number of elements. As stated earlier, the number of array elements for Simulator # 1 is one and one-half. In practice, fractional elements can often be omitted with negligible error in the simulator. Figure 5 shows the schematic diagram of Simulator # 1. The left-hand side shows Simulator # 1 without an excitation waveguide. The probe is made up of a very thin rectangular metal filament (of length l) supported by a rectangular piece of duroid (a dielectric material). The right-hand side shows the simulator waveguide. Since the simulator waveguide is a nonstandard waveguide, a standard S-band waveguide is used for excitation. To match the S-band waveguide to the simulator waveguide, a tapered section is used, as shown in Fig. 5. The center of that figure shows a rectangular dielectric piece of thickness t. This dielectric piece will simulate Munk's proposed dielectric sheet that is in front of the array face for aperture matching [12].

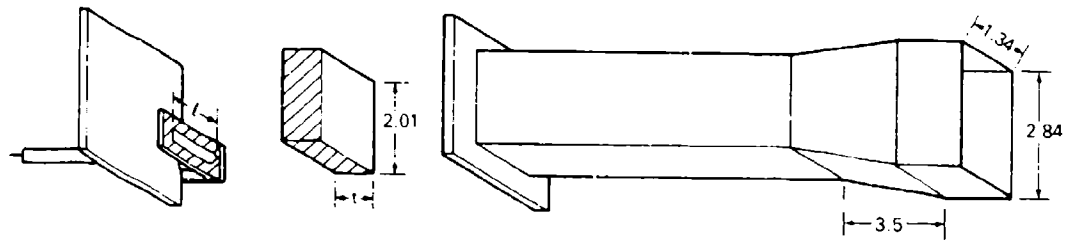

ALL DIMENSIONS ARE IN INCHES

Fig. 5 — Schematic diagram of Simulator # 1

Figures 6 and 7 show the schematic diagrams of two other H-plane simulators. The simulator in Fig. 6 contains two and one-half elements, and the simulator in Fig. 7 contains five elements. The scan angles represented by those simulators as a function of frequency were shown in Fig. 2. Figure 8 shows these three H-plane simulators. Since Simulator # 1 contains only one full element, it is possible not only to measure input VSWR, but also the active input impedance. With the other two simulators, only the input VSWR was measured.

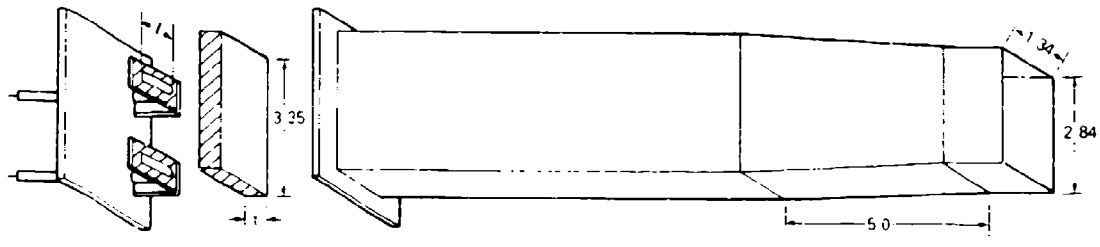

ALL DIMENSIONS ARE IN INCHES

Fig. 6 — Schematic diagram of Simulator # 2

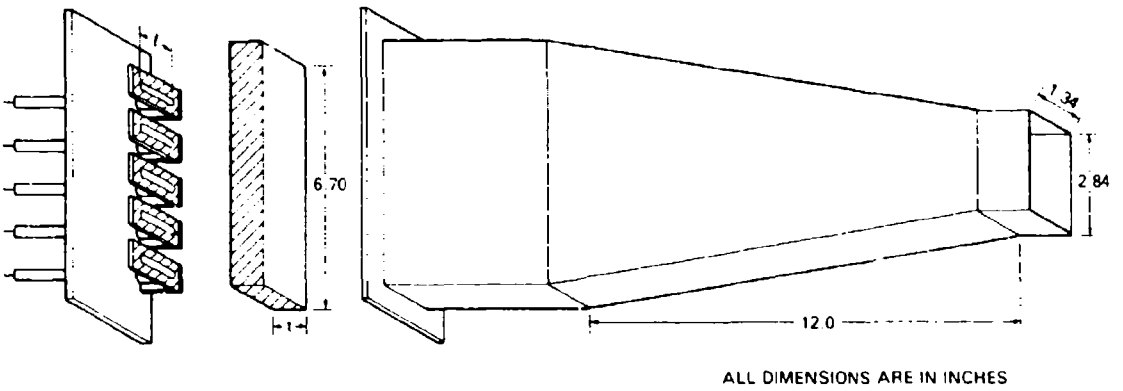

Fig. 7 – Schematic diagram of Simulator #3

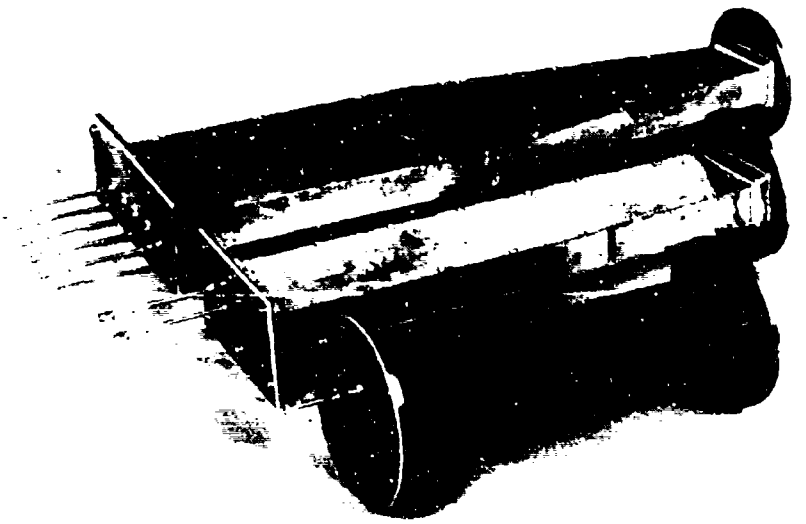

Fig. 8 — Three H-plane simulators

Figure 9 shows the VSWR vs frequency for Simulator #1. The results have peaks and valleys. The reason for these variations was found to be due to the reflections from the ends of the tapered section of Simulator #1 because of its finite length. Instead of building another simulator with a longer tapered section, the reflections at each frequency of interest were tuned out by using metallic screws before the VSWR and active input impedance measurements were made. Figures 10 and 11 show the results. The variations of VSWR and input impedance are much smaller, indicating the absence of reflections from the tapered waveguide section. These measurements were for a thin metallic probe supported in the back by a rectangular piece of duroid. Figure 12 shows VSWR vs frequency for all three H-plane simulators. To compare the results, measurements were also made by using a thick (10 mils) metallic probe with no dielectric backing, and the results are shown in Fig. 13. The results from Figs. 12 and 13 indicate that the thin probe with dielectric backing gave better results. The maximum VSWR over the whole frequency range of interest is 2.35 with dielectric backing and 3.1 without dielectric backing of the probes. Since the dielectric backing for the probes gave better results, it was decided to increase the dielectric backing to occupy the full cross section of the waveguide simulator. It was reasoned that if this configuration were to be successful, it will be much easier to build an array because the probe elements can be built by using metallic deposition on

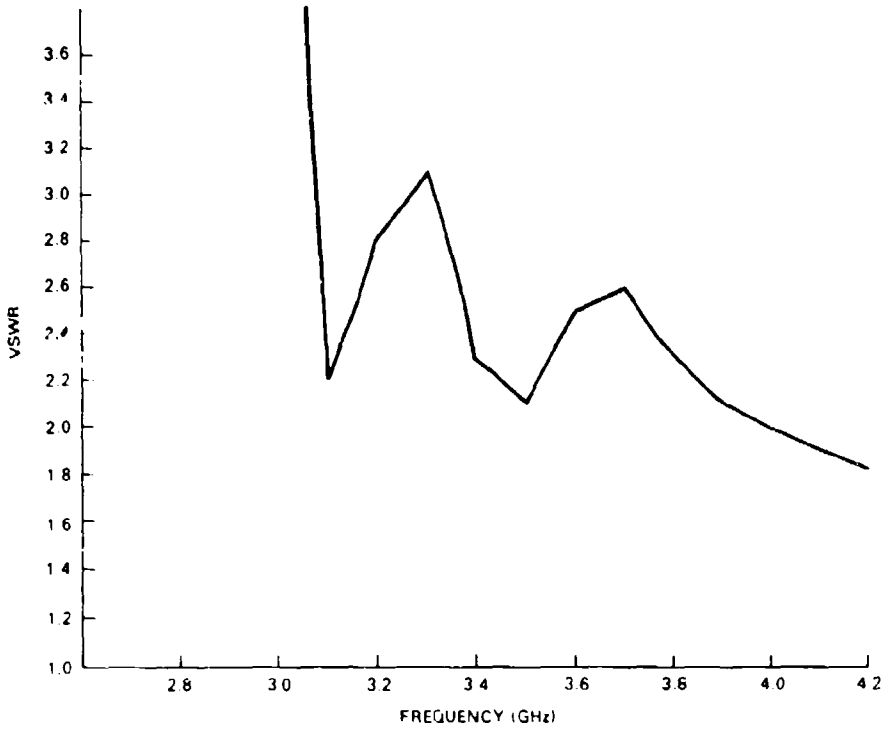

Fig. 9 — VSWR of the element in Simulator #1 with short tapered waveguide section

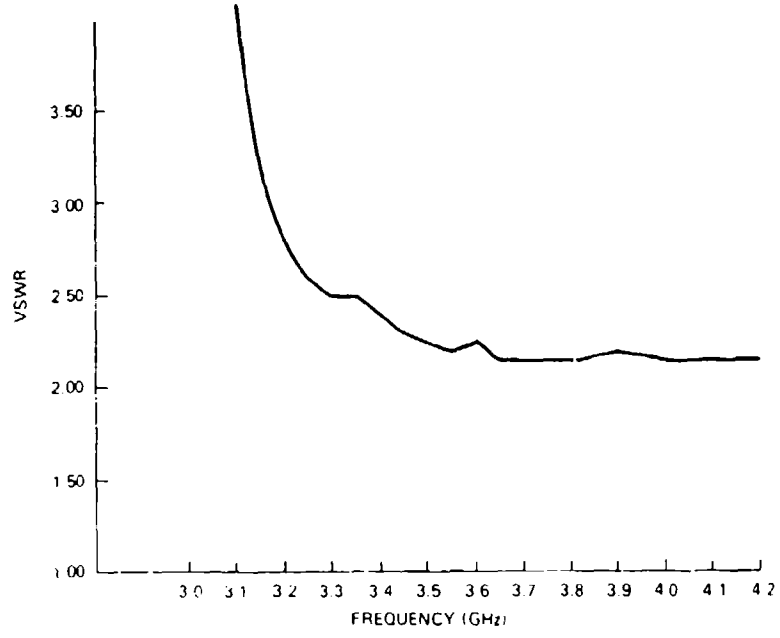

Fig. 10 — VSWR of the element in Simulator #1 with reflections from the tapered section tuned out

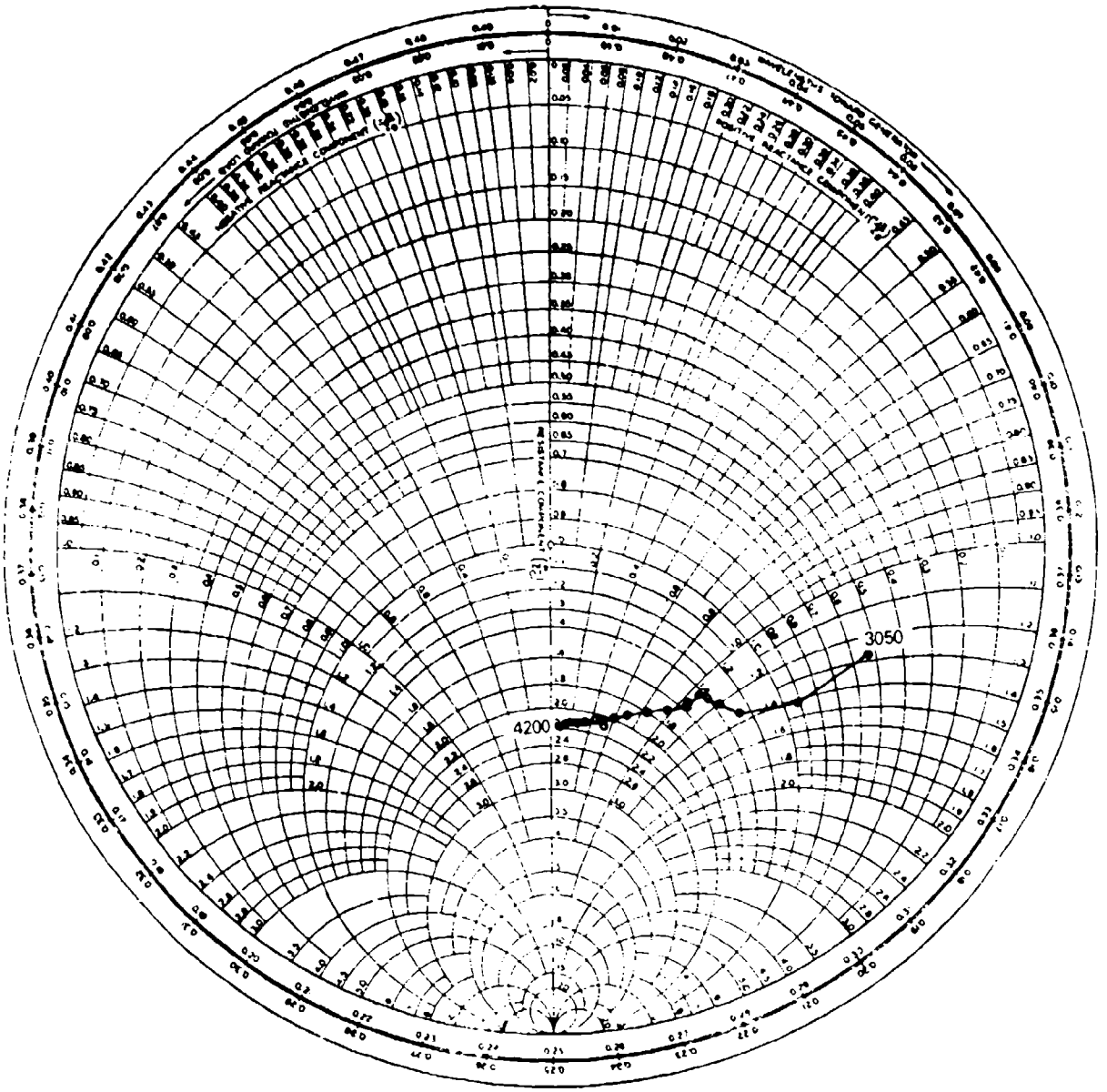

Fig. 11 — Input impedance of the element in Simulator #1 with reflection from the tapered section tuned out

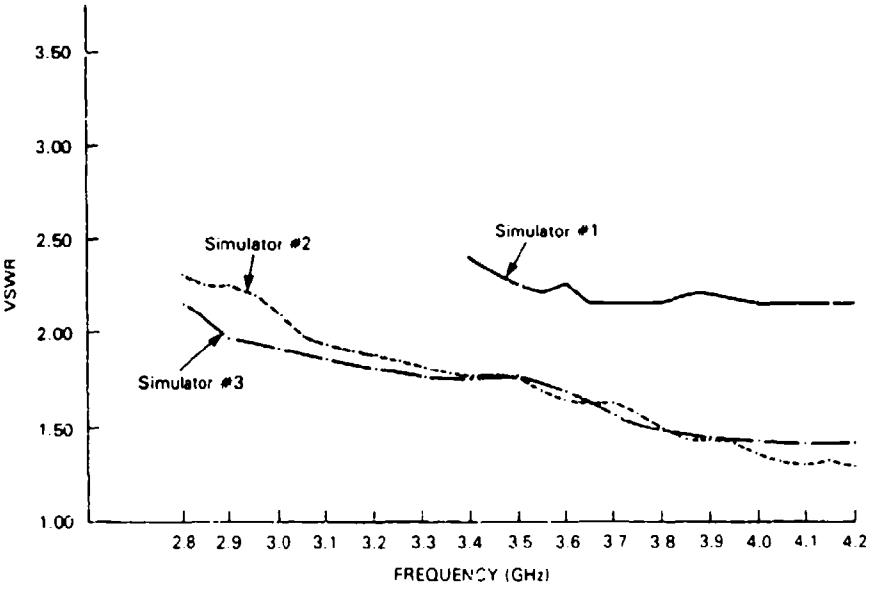

Fig. 12 — VSWR vs frequency for three H-plane simulators when the thin metallic strip probes are supported in the back by rectangular pieces of dielectric material

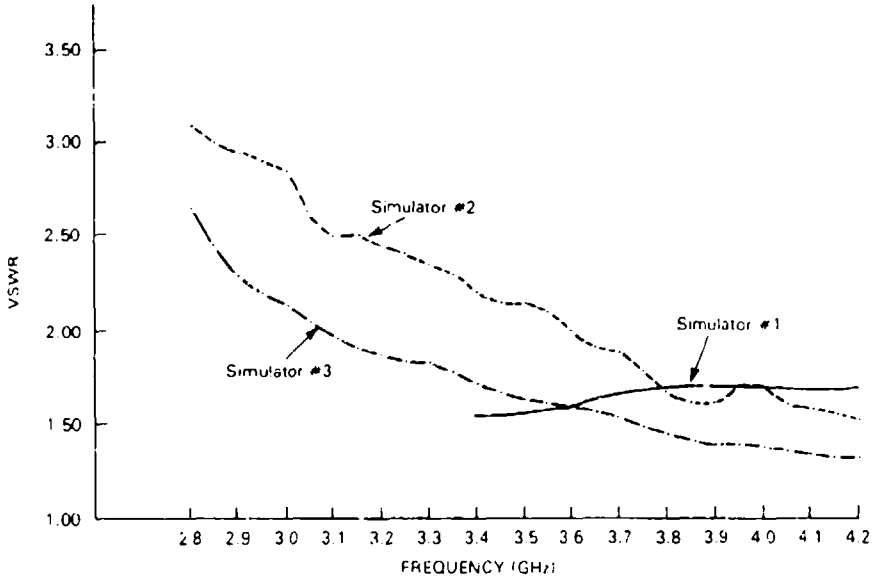

Fig. 13 — VSWR vs frequency for three H-plane simulators when 10-mils-thick metallic strips are used as probes

dielectric sheet (as will be discussed later). Figure 14 shows the results of VSWR as a function of frequency for three H-plane simulators when the dielectric backing occupied the full cross section of the waveguide simulators. The VSWR curve for Simulator #1 has improved, especially at the high-frequency end compared to the results shown in Fig. 12. Simulator #3 results have also improved, but at the low frequency end. There is no noticeable change for Simulator #2. However, the maximum VSWR over the full frequency range is still 2.35 and did not degrade. Therefore, for convenience of design, the remaining experiments with the waveguide simulators were done with the probes supported by a full dielectric sheet.

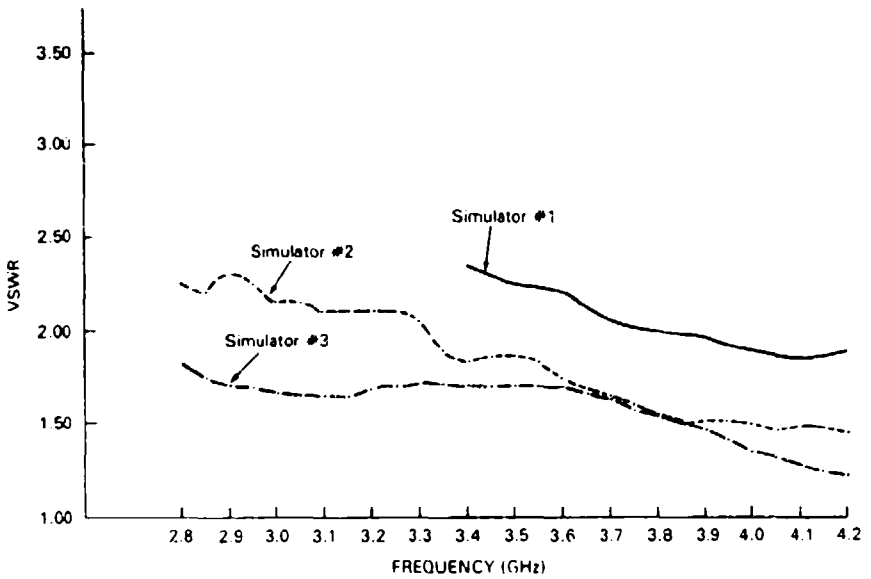

Fig. 14 — VSWR vs frequency for three H-plane simulators with thin metallic strip probes supported in the back by a thin dielectric sheet

Munk [12] proposed the use of a low dielectric constant slab in front of, and adjacent to, a phased array, as a technique to improve aperture matching over a large scan angle. According to Munk [12], the slab dielectric constant ϵ_r and the slab thickness d are given by

$$\epsilon_r = 1 + \cos\theta_0 \tag{3}$$

and

$$d = \frac{\lambda_e}{4} \frac{1}{\cos\theta_e} \tag{4}$$

where θ_0 is the chosen optimum scan angle ($<90°$), for which the aperture is perfectly matched,
λ_e is the wavelength in the dielectric slab,
and $\sin\theta_e = \sin\theta_0/\epsilon_r$.

For $\epsilon_r = 1.3$ and center frequency of 3.5 GHz, the slab thickness d is calculated to be 1.09 in. Munk, however, did not address the problem of broader bandwidths in his analysis. In the experimental work presented here, different slab thicknesses were evaluated for improving bandwidth performance.

The placement of the dielectric slab in front of the probes was varied. The best results were obtained, however, when the slab is against the probes. The results presented here correspond to this configuration only.

Figures 15 and 16 show results with slab thickness of 1 and 0.5 in., respectively. The best results were obtained with a thickness of 0.5 in. with an increase in probe length to 0.7 in. Figure 17 shows these results. Increasing the probe length decreased the VSWR on the low-frequency side for Simulators #2 and #3. It increased the VSWR for Simulator #1. The maximum VSWR for all the simulators over the complete frequency range is 2.1. This is very close to our original goal of 2 over a 40% bandwidth.

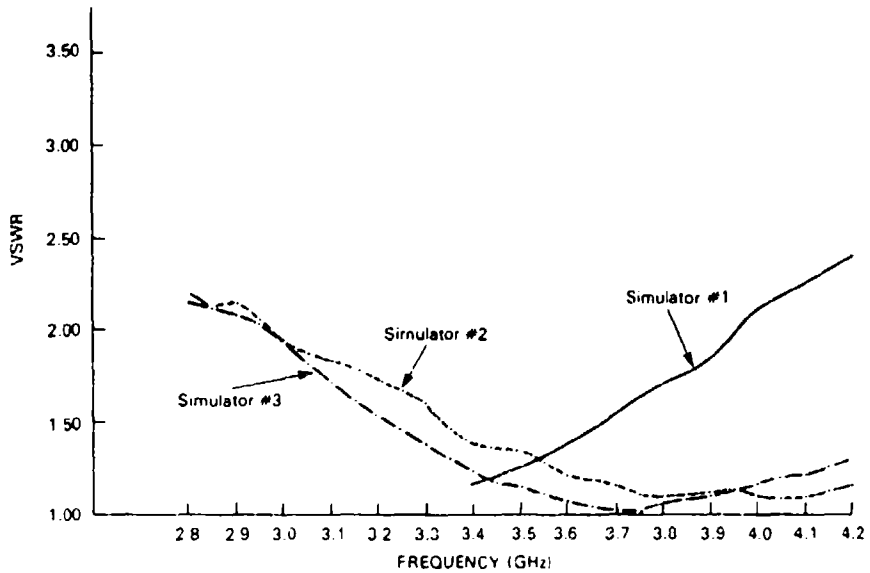

Fig. 15 — VSWR vs frequency for three H-plane simulators with dielectric loading (slab thickness = 1 in. $\epsilon_r = 1.3$) and probes length $l = 0.65$ in.

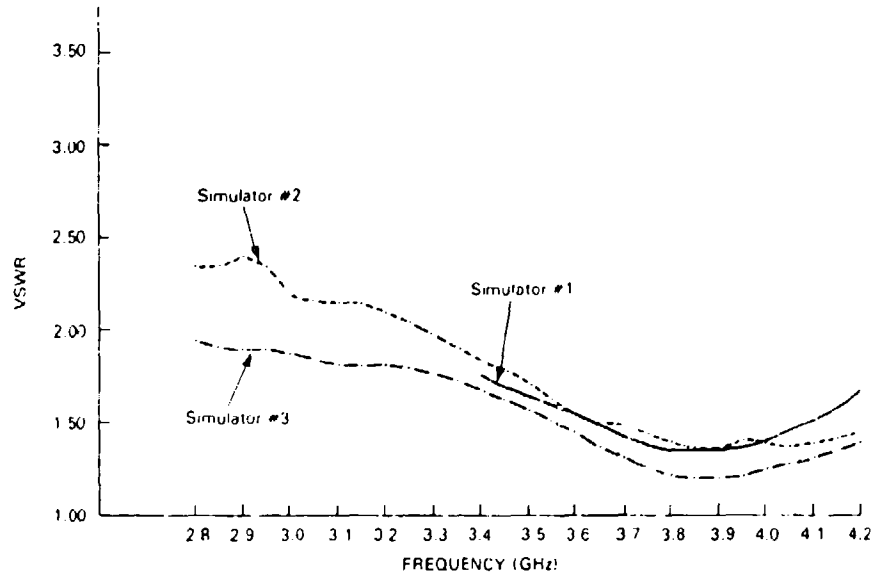

Fig. 16 — VSWR vs frequency for three H-plane simulators with dielectric loading (slab thickness = 0.5 in., $\epsilon_r = 1.3$) and probes length $l = 0.65$ in.

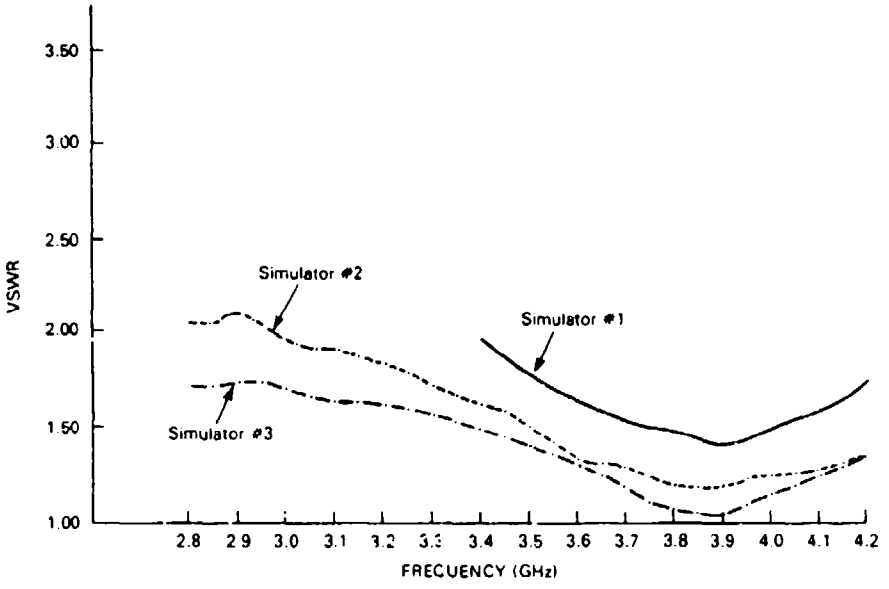

Fig. 17 — VSWR vs frequency for three H-plane simulators with dielectric loading (slab thickness = 0.5 in., $\epsilon_r = 1.3$) and probes length $l = 0.7$ in.

Experimental Array

The results of the three simulators indicated the performance of the infinite array at only three discrete scan angles over the frequency range of interest. To obtain additional information on scan performance, a small array was built to measure the central element pattern, with all the other elements terminated in matched load. If the aperture matching is perfect, the measured element pattern will have a cosine variation with scan angle θ [13]. If the aperture matching is not perfect, the normalized element power pattern is given by [13]

$$F(\theta,\phi) = \frac{D_x D_y}{\lambda^2} \cos\theta \, (1 - |\Gamma(\theta,\phi)|^2) \tag{5}$$

where D_x and D_y are interelement spacings in rectangular coordinates x and y, θ and ϕ are polar coordinates, and $\Gamma(\theta,\phi)$ is the element active-reflection coefficient.

From Eq. (5) and knowing the element pattern, the magnitude of the active-reflection coefficient can be determined at any scan angle of interest. By repeating the experiment at different frequencies, the array-aperture matching (active-reflection coefficient) can be found over the required frequency and scan ranges. This is the motivation in building and making measurements on an 11 × 11 array. The optimized array parameters, as determined from simulator experimental results were used in building the 11 × 11 element array. Figure 18 shows the sketch of the array. The probe length is 0.7 in. The probes are etched (or deposited) on a thin duroid sheet. The individual probes are fed by 50 Ω coaxial lines. The parallel plates are extended beyond the probe location. Dielectric slabs, inserted in front of the probes (and in between parallel plates), have also been used to improve aperture matching. Parallel plate septa were first built to extend one inch beyond the probe locations. Figure 19 shows the picture of the experimental array (with no dielectric loading). Additional extensions of parallel plates to 1-1/2 and 2 in. were achieved by attaching additional metal plates.

The active element pattern of the central element was measured after terminating the rest of the input coaxial lines with 50 Ω loads. Preliminary results indicated that the finiteness of the array, especially the abrupt ending of the parallel plates on the sides, caused ripples in the measured element-radiation pattern. The use of absorbing material around the array improved the situation.

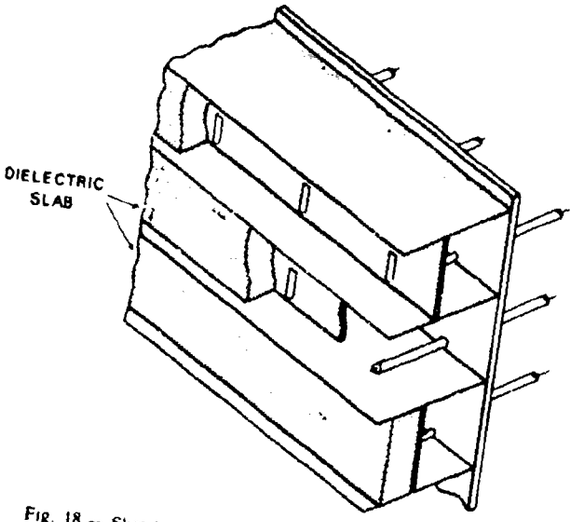

Fig. 18 — Sketch of the 11 × 11 element experimental array

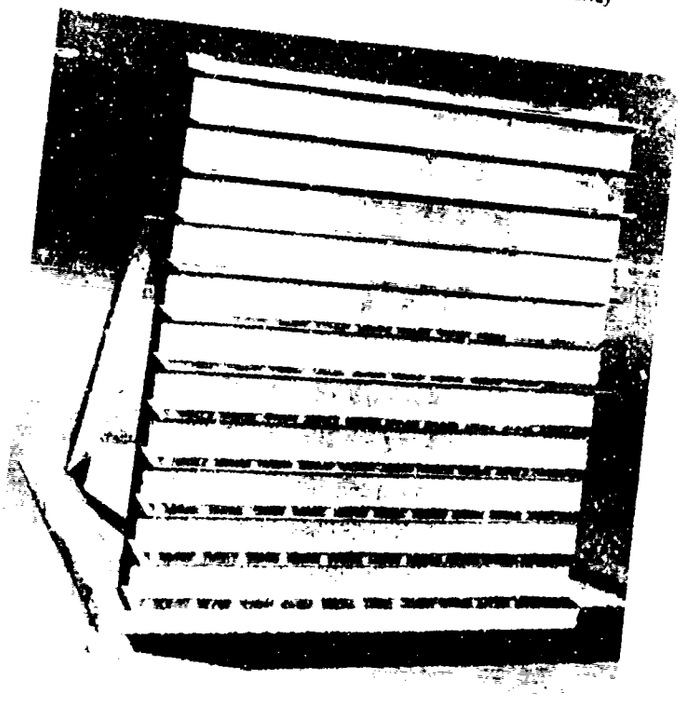

Fig. 19 — Actual experimental array 81599-2

However, the measurement results depended on the location and placement of the absorbing material, and the results were not repeatable with any accuracy better than ± 0.5 dB. For this reason, the parallel plates were extended by about 4 in. on both sides of the array and were completely filled with absorbing material. Additional absorbing material of about 12 in. wide was also used on all four sides of the array.

Figures 20 and 21 show the active element patterns (patterns of the central element when all the other elements are terminated in matched loads), in the H- and E-plane, respectively, when the parallel plates are extended to 1 in. beyond the position where the probes are located (but with no dielectric loading). These are the measured patterns for each of several frequencies evenly spaced over the frequency band of interest (2.8 to 4.2 GHz). The patterns are shown for an angular range slightly greater than $\pm 60°$. However, our interest is mainly up to $\pm 60°$. If the aperture matching is perfect, the pattern will be down to -3 dB at $\pm 60°$, because as stated before, the active element pattern should be a cosine function (as noted from Eq. (5) with $\Gamma = 0$). For a mismatch with VSWR $\leqq$ 2, the reflection coefficient $\Gamma \leqq 1/3$. Substituting the value for $\Gamma = 1/3$ in Eq. (5), one shows that the element pattern should be down to only -3.5 dB. The patterns in Figs. 20 and 21, however, are down to -5 dB at 4.2 GHz for H-plane scanning and at 3.6 GHz for E-plane scanning. There are at least two reasons for this. The first reason is the contribution owing to aperture mismatch, and the other is the pattern ripples contributed by the finiteness of the array [14] and the location of the absorbing material around the antenna array. The pattern ripples depended on the location of the absorbing material whenever the antenna-array setup was changed to make pattern measurements in different planes. Our measurements revealed that it was impossible to repeat patterns in any plane with an accuracy better than ± 0.5 dB. Therefore, even if the element pattern is down to -4 dB at $\pm 60°$, the aperture could be well matched with VSWR $\leq$ 2. The element patterns shown in Figs. 20 and 21, however, are down to -5 dB at some frequencies, indicating a mismatch with VSWR $\geq$ 2. To improve the aperture match, a dielectric slab, initially 1 in. thick and with $\epsilon_r = 1.3$, was inserted between the parallel plates. Figures 22 and 23 show the H- and E-plane active element patterns with dielectric slab loading. The H-plane patterns are down to only -4 dB at all frequencies except 4.2 GHz. In the E-plane also, the patterns improved except at 4.2 GHz where the pattern became very poor. Results improved when the dielectric slab thickness is reduced to 0.5 in. The patterns so obtained are shown in Figs. 24 and 25. The H-plane patterns are down to about -4 dB at some frequencies when scanned to $\pm 60°$. At many other frequencies, the patterns are down to only 3 dB, which indicate good aperture match. As noted before, the waveguide-simulator results showed that the aperture is well matched, with VSWR of about 2:1 for H-plane scanning. The E-plane patterns shown in Fig. 25 are no worse than H-plane patterns shown in Fig. 24, indicating a good aperture match even for E-plane scanning.

To determine the effect of the parallel-plate septa, the active element radiation patterns were taken by extending the parallel plates to 1.5 in. and then to 2.0 in. in front of the probes, instead of the original 1.0 in. Patterns were taken with and without dielectric loading. The results revealed that the 1 in. length for the parallel-plate septa is about the best value. Therefore, no additional results are presented.

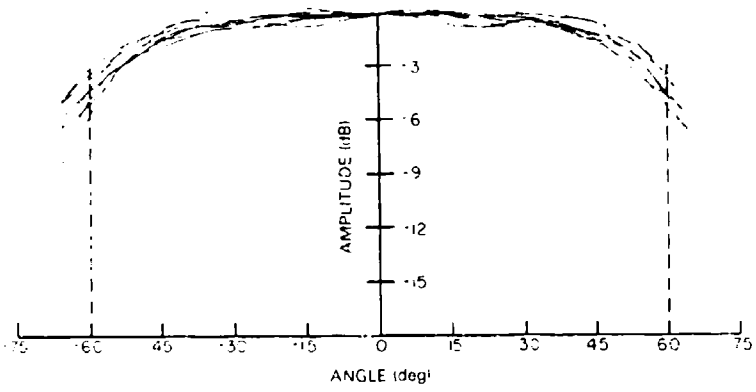

Fig. 20 — H-plane active element pattern when parallel-plate septa length = 1 in. and no dielectric loading

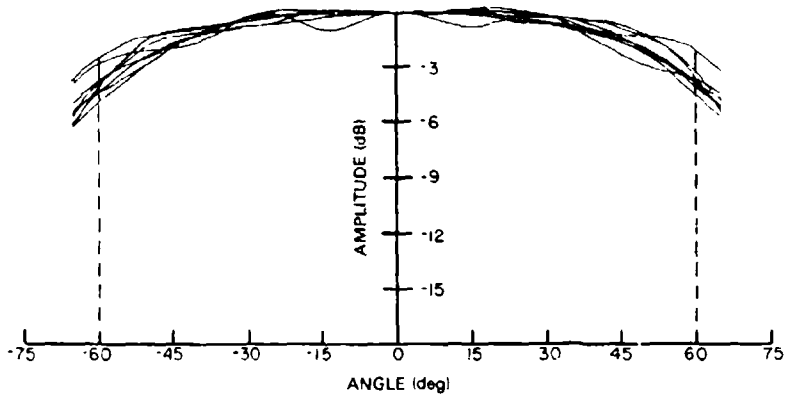

Fig. 21 — E-plane active element pattern when parallel-plate septa length = 1 in. and no dielectric loading

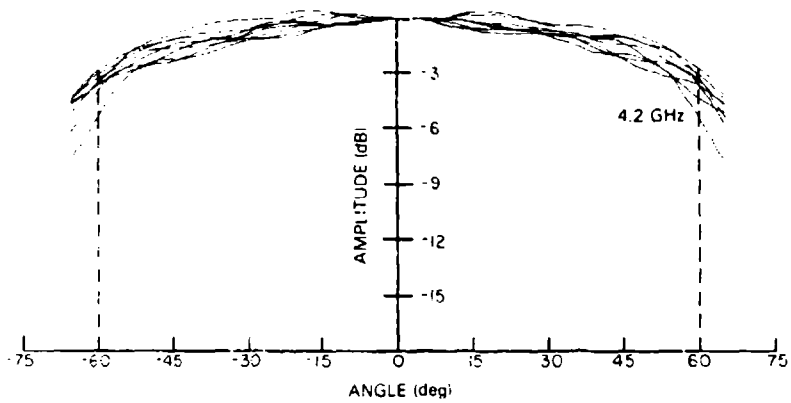

Fig. 22 — H-plane active element pattern with 1 in. dielectric slab loading

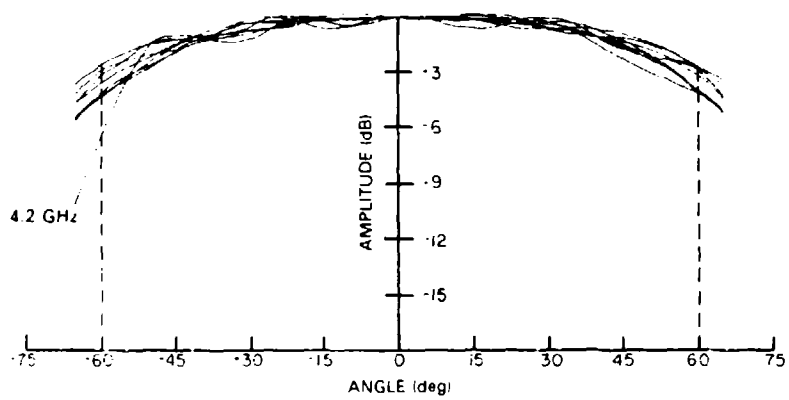

Fig. 23 — E-plane active element pattern with 1 in. dielectric slab loading

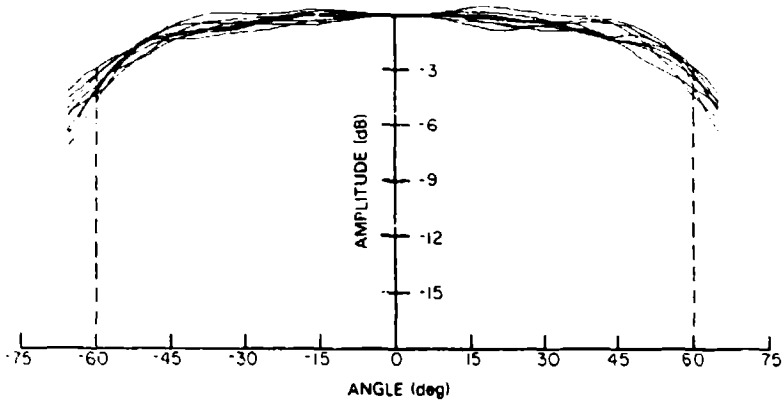

Fig. 24 — H-plane ... e element pattern with 0.5 in dielectric slab loading

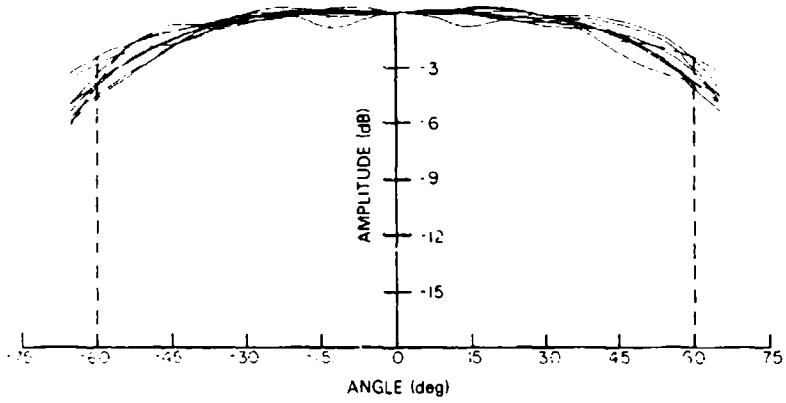

Fig. 25 — E-plane active element pattern with 0.5 in ... electric slab loading

DISCUSSION AND CONCLUSIONS

This report covers the experimental work conducted on the design and development of a broadband, wide angle scanned phased array. A parallel-plate waveguide element was used as the radiating element. Three H-plane waveguide simulators were built and used to optimize the array parameters to improve frequency and scanning performance. The experimental results obtained by using the waveguide simulator showed that the aperture VSWR of less than 2.1 was achieved over a 40% frequency bandwidth and for scan range of $\pm 60°$. Experimentally optimized array parameters are then used to build an 11 × 11 element array. The scanning performance of this array in H- and E planes was studied by measuring active element patterns. The measured results showed that the aperture match is equally good with estimated VSWR of about 2 over $\pm 60°$ scan range and over 40% bandwidth for H- and E-plane scanning.

REFERENCES

1. A.A. Oliner and G.H. Knittel, eds., *Phased Array Antennas* (Artech House, Dedham, MA, 1972).

2. N. Amitay, V. Galindo, and C.P. Wu, *Theory and Analysis of Phased Array Antennas* (Wiley Interscience, New York, 1972).

3. R.C. Hansen, ed., *Significant Phased Array Papers* (Artech House, Dedham, MA, 1973).

4. M.I. Skolnik, *Radar Handbook* (McGraw-Hill, Inc., New York, 1970), pp. 11-1 to 11-71.

5. R.C. Hansen, ed., *Microwave Scanning Antennas* (Academic Press, New York, 1966).

6. R.J. Mailloux, J.F. McIlvenna, and N.P. Kernweis, "Microstrip Array Technology," *IEEE Trans. Antennas Propag.*, **29**(1), 25-37 (1981).

7. S.N. Samaddar, "Input Impedance of an Infinite Linear Scanned Array of Flat Rectangular Strips Inside a Dielectric Loaded Parallel Plate Waveguide," NRL Memorandum Report 5830, July 1986.

8. P.W. Hannan and M.A. Balfour, "Simulation of a Phased Array Antenna in Waveguide," *IEEE Trans. Antennas Propag.* **13**, 342-353 (1965).

9. H.A. Wheeler, "A Survey of the Simulator Technique for Designing a Radiating Element in Phased Array Antenna," in *Phased Array Antennas*, A.A. Oliner and G.H. Knittel, eds. (Artech House, Dedham, MA, 1972), pp. 132-148.

10. D. Davis, G.E. Evans, V.L. Fisher, and A.H. Johnson, "Development of Scanning Dipole Array," Westinghouse Electric Corporation Report (private communication).

11. P.D. Hrycak, "Multimode Simulator Techniques Used In the Design of a Scanning Radiating Element," 1983 Int. Symp. Antennas Propag. **2**, 381-384, 1983.

12. B.A. Munk, T.W. Kornbau and R.D. Fulton, "Scan Independent Phased Arrays," *Radio Sci.* **14**(6), 979-990 (1979).

13. W. Wasylkiwskyj, and W.K. Kahn, "Element Patterns and Active Reflection Coefficient in Uniform Phased Arrays," *IEEE Trans. Antenna Propag.* **AP-22** (2), 207-212 (1974).

14. W.K. Kahn, "Impedance-Match and Element-Pattern Constraints for Finite Arrays," *IEEE Trans. Antennas Propag.* **25**(6), 747-755 (1977).

BIBLIOGRAPHY

Phased Array Antennas

1. Cheston, T.C., "Beam Steering of Planar Phased Arrays," in *Phased Array Antennas*, A.A. Oliner and G.H. Knittel, eds. (Artech House, Dedham, MA, 1972), pp. 219-221.

2. Davis, D., "Slot Element Analysis and Design," DESC-12213, Westinghouse Electric Corporation Report, Jan. 1981.

3. Diamond, B.L., "Small Arrays—Their Analysis and Their Use for the Design of Array Elements," in *Phased Array Antennas*, A.A. Oliner and G.H. Knittel, eds. (Artech House, Dedham, MA, 1972), pp. 127-131.

4. Frazita, R.F., "Surface Wave Behavior of a Phased Array Analyzed by Grating-Lobe Series," *IEEE Trans. Antenna Propag.* **15**, 823-824 (1967).

5. Hannan, P.W., "The Element-Gain Paradox of a Phased-Array Antenna," *IEEE Trans. Antennas Propag.* **12**, 423-433 (1964).

6. Hannan, P.W., "Proof That a Phased Array Antenna Can Be Impedance Matched at All Scan Angles," *Radio Sci.* **2**(3) (new series), 361-369 (1967).

7. Kahn, W.K., "Impedance Match and Element-Pattern Constraints for Finite Arrays," *IEEE Trans. Antennas Propag.* **25**(6), 747-755 (1977).

8. Lewis, L.R., M. Fassett and J. Hunt, "A Broadband Stripline Array Element," Digest of the International Symposium of Antennas and Propagation, Atlanta, GA, June 1974, pp. 335-337.

9. Mailloux, R.J., "Surface Waves and Anomalous Wave Radiation Nulls on Phased Arrays of TEM Waveguides with Fences," *IEEE Trans. Antennas Propag.* **20**, 160-166 (1972).

10. Van Schaik, H.J., "Numerical and Experimental Antenna Patterns of a Planar Space-Fed, Phased Array Antenna," International Conference on Antennas and Propagation, IEE Conference Publication No. 169, Nov. 1978, pp. 11-15.

11. Von Aulock, W.H., "Properties of Phased Arrays," *Proc. IRE*, **48**, 1715-1727 (1960).

12. Wasylkiwskyj, W. and W.K. Kahn, "Theory of Mutual Coupling Among Minimum-Scattering Antennas," *IEEE Trans. Antennas Propag.* **18**(2), 204-216 (1970).

13. Wasylkiwskyj, W. and W.K. Kahn, "Infinite Array of Sub-array Antennas," in *Phased Array Antennas*, A.A. Oliner and G.H. Knittel, eds. (Artech House, Dedham, MA, 1972), pp. 83-90.

14. Wasylkiwskyj, W. and W.K. Kahn, "Element Pattern Bounds in Uniform Phased Arrays," *IEEE Trans. Antennas Propag.* **25**(5), 597-604 (1977).

15 Wheeler, H.A., "The Grating-Lobe Series for the Impedance Variation in a Planar Phased Array Antenna," *IEEE Trans. Antennas Propag.* **14**, 707-714 (1966).

16. Wheeler, H.A., "A Systematic Approach to the Design of a Radiator Element for a Phased-Array Antenna," *Proc. IEEE* **56**(11), (1968).

17. Zaghloul, A.I., "Matching Networks in Linear Phased Array," *Comsat Technical Rev.* **13**(1), 71-86 (1983).

WAIM — Phased Arrays

1. Byron, E.V. and J. Frank, "On the Correlation Between Wide-Band Arrays and Array Simulators," *IEEE Trans. Antennas Propag.* **16**, 601-603 (1968).

2. Chen, C.C., "Broadband Impedance Matching of Rectangular Waveguide Phased Array," *IEEE Trans. Antennas Propag.* **21**(3), 298-302 (1973).

3. Cheston, T.C., "On the Matching of Phased Array Antenna," *IEEE Trans. Antennas Propag.* **13**, 327, (1965).

4. Kelly, A.J., "Comments on 'Wide-Angle Impedance Matching of a Planar Array Antenna by a Dielectric Sheet'," *IEEE Trans. Antennas Propag.* **14**, 636-637 (1966).

5. Magill, E.G. and H.A. Wheeler, "Wide-Angle Impedance Matching of a Planar Array Antenna by a Dielectric Sheet," *IEEE Trans. Antennas Propag.* **14**(1), 49-53 (6).

6. Snieder, J., "A Simple and Fast Matching Method for M ual Coupling of a Linear Phased Array Antenna with Waveguide Apertures as Radiating Elements," International Conference Radar-77, IEE Conference Publication No. 156, Oct. 1977, pp. 432-436.

7. Snieder, J., "The Design, Construction and Test Results of the CAISSA Planar Space Fed Phased Array Antenna," Proc. of the First Military Microwave Conference, Oct. 1978, pp. 391-402.

8. Van Schaik, H.J., "Theoretical and Experimental Results of an Iris-Loaded Planar Phased-Array Antenna with an External Dielectric Sheet," International Conference Radar-77, IEE Conference Publication No. 155, pp. 437-441, Oct. 1977.

9. Van Schaik, H.J., "The Performance of an Iris-Loaded Planar Phased Array Antenna of Rectagular Waveguides with an External Dielectric Sheet," *IEEE Trans. Antennas Propag.* **26**(3), 413-419 (1978).

Simulators

1. Balfour, M.A., "Phased Array Simulators in Waveguides for a Triangular Arrangement of Elements," *IEEE Trans. Antennas Propag.* **13**, 475-476 (1965).

2. Balfour, M.A., "Active Impedance of a Phased-Array Antenna Element Simulated by a Single Element in Waveguide," *IEEE Trans. Antennas Propag.* **15**(2), 313-314 (1967).

3. Brown, C.R. and T.F. Carberry, "A Technique to Simulate the Self and Mutual Impedances of an Array," *IEEE Trans. Antennas Propag.* **14**, 377-378 (1968).

4. Gustincic, J.J., "The Determination of Active Array Impedance with Multi-Element Waveguide Simulators," *IEEE Trans. Antennas Propag.* **20**(5), 589-595 (1972).

5. Hannan, P.W., P.J. Meier, and M.A. Balfour, "Simulation of Phased Array Antenna Impedance in Waveguide," *IEEE Trans. Antennas Propag.* **11**, 715-716 (1963).

6. Hannan, P.W., "Discovery of an Array Surface Wave in a Simulator," *IEEE Trans. Antennas Propag.* **15**, 574-576 (1967).

Probe in a Waveguide

1. Biakowski, M.E. and P.J. Kahn, "Determination of the Admittance of a General Waveguide-Coaxial Line Junction," *IEEE Trans. Microwave Theory Tech.* **32**(4), 465-467 (1984).

2. Chien, W.Z., L. Infeld, J.R. Pounder, A.F. Stevenson, and J.L. Synge, "Contributions to the Theory of Waveguides," *Can. J. Res.* **27**, Sec. A, 69-127 (1949).

3. Collin, R.E., *Field Theory of Guided Waves* (McGraw-Hill, New York, 1960), pp. 258-271.

4. Eisenhart, R.L., P.T. Grieling, L.K. Roberts, and R.S. Robertson, "A Useful Equivalence for a Coaxial-Waveguide Junction," *IEEE Trans. Microwave Theory Tech.* **26**(3), 172-174 (1978).

5. Friedman, D.S., "Optimum Bandwidth for Waveguide-to-Coaxial Transducers," *IRE Trans. Microwave Theory Tech.* **5**, 75 (1957).

6. Lewin, L., "A Contribution to the Theory of Probes in Waveguides," *Proc. IEE* **105**, Pt. C, 109-116 (1958).

7. Mumford, W.W., "The Optimum Piston Position for Wide-band Coaxial-to-Waveguide Transducers," *Proc. IRE* **41**, 256-261 (1953).

8. Wheeler, G.J., "Broadband Waveguide-to-Coax Transitions," IRE National Convention Record, Pt. 1, Mar. 1957, pp. 182-185.

9. Williamson, A.G. and D.V. Otto, "Cylindrical Antenna in a Rectangular Waveguide Driven from a Coaxial Line," *Electron. Lett.* **8**(22), 545-547 (1972).

10. Williamson, A.G. and D.V. Otto, "Coaxially Fed Hollow Cylindrical Monopole in a Rectangular Waveguide," *Electron. Lett.* **9**(10), 218-220 (1973).

11. Williamson, A.G. and D.V. Otto, "Analysis of a Waveguide Mounting Structure," *Proc. IREE* **34**, 95-97 (1973).

12. Williamson, A.G., "Analysis and Modelling of a Coaxial-Line/Rectangular-Waveguide Junction," *Proc. IEE* **129**, Pt. H, 262-270 (1982)